Approaches to unravel seasonality in sea surface temperatures using paired single-specimen foraminiferal $\delta^{18}O$ and Mg/Ca analyses

J. C. Wit,[1] G.-J. Reichart,[1,2] S. J. A Jung,[3] and D. Kroon[3,4]

Received 4 September 2009; revised 29 July 2010; accepted 2 September 2010; published 7 December 2010.

[1] Seasonal changes in surface ocean temperature are increasingly recognized as an important parameter of the climate system. Here we assess the potential of analyzing single-specimen planktonic foraminifera as proxy for the seasonal temperature contrast (seasonality). Oxygen isotopes and Mg/Ca ratios were measured on single specimens of *Globigerinoides ruber*, extracted from surface sediment samples of the Mediterranean Sea and the adjacent Atlantic Ocean. Variability in $\delta^{18}O$ and Mg/Ca was then compared to established modern seasonal changes in temperature and salinity for both regions. The results show that (1) average $\delta^{18}O$-derived temperatures correlate with modern annual average temperatures for most sites, (2) the range in $\delta^{18}O$- and Mg/Ca-derived temperature estimates from single-specimen analysis resembles the range in seasonal temperature values at the sea surface (0–50 m) in the Mediterranean Sea and the Atlantic Ocean, and (3) there is no strong correlation between Mg/Ca- and $\delta^{18}O$-derived temperatures from the same specimens in the current data set, indicating that other parameters (salinity, carbonate ion concentration, symbiont activity, ontogenesis, and natural variability) potentially affect these proxies.

Citation: Wit, J. C., G.-J. Reichart, S. J. A Jung, and D. Kroon (2010), Approaches to unravel seasonality in sea surface temperatures using paired single-specimen foraminiferal $\delta^{18}O$ and Mg/Ca analyses, *Paleoceanography*, *25*, PA4220, doi:10.1029/2009PA001857.

1. Introduction

[2] A considerable amount of paleoclimate literature has focused on past changes in annual temperature. However, seasonal variations in temperature can be orders of magnitude larger than interannual variations, and both may be crucial to understanding past climate change. For example, *Denton et al.* [2005] showed that the onset of the Younger Dryas event involved an abrupt decrease in mainly winter temperatures, resulting in a major shift in seasonal temperature contrast. Somewhat analog, the Mg/Ca from planktonic foraminifera, in cores from the Caribbean, covering the Last Glacial Maximum and Termination I, showed an increase in seasonal temperature contrast, due to deteriorating winter conditions [*Ziegler et al.*, 2008]. These interpretations of the seasonal temperature contrast are tentative, because calibrated and direct proxies for seasonality are lacking.

[3] Stable oxygen isotope and Mg/Ca values in shells of planktonic foraminifera are standard tools to unravel the average temperature history of the surface ocean [*Shackleton*, 1974; *Bemis et al.*, 1998; *Lea et al.*, 1999; *Elderfield and Ganssen*, 2000]. Previous studies, however, rarely assessed the seasonal aspect within these proxies. Seasonal variations in precipitation/evaporation control the $\delta^{18}O_{(water)}$ and salinity of seawater, whereas temperature controls fractionation of stable isotopes during carbonate formation. The $\delta^{18}O$ in foraminifera, therefore, represents $\delta^{18}O_{water}$ and temperature, while Mg/Ca values mainly reflect the temperature of the ambient seawater [e.g., *Epstein et al.*, 1951; *Shackleton*, 1974; *Elderfield and Ganssen*, 2000; *Anand et al.*, 2003]. Hence, seasonal variations in sea surface temperatures should be reflected in the $\delta^{18}O$ and Mg/Ca values of individual specimens, as they reflect environmental conditions during calcification through the year. Applied to deep sea sediments, variability in $\delta^{18}O$ and Mg/Ca between individual specimens of one sample would be indicative for the seasonal temperature range depending on bioturbation and sedimentation rate.

[4] Due to the geographic location and its enclosed nature, the Mediterranean experiences large seasonal changes reflecting the alternating influence of the African monsoon and more temperate parts of the northern hemisphere climate system [*Rossignol-Strick*, 1985, and references therein; *Hurrell*, 1995], thus forming an ideal environment for testing this potential proxy for seasonality. In order to test the wider use of the method outside the Mediterranean Sea, a site from the North Atlantic was also examined. This site is contrasting to the Mediterranean and has smaller seasonal variations due to the open ocean environment. *Globigerinoides ruber* is a shallow dwelling (0–50 m) spinose species mainly living in oligotrophic waters [*Hemleben et al.*, 1989]. Because of its shallow habitat this species has been used to reconstruct sea

[1]Department of Geochemistry, Faculty of Geosciences, Utrecht University, Utrecht, Netherlands.
[2]Alfred Wegener Institute for Polar and Marine Research, BioGeoScience, Bremerhaven, Germany.
[3]School of GeoSciences, Grant Institute, University of Edinburgh, Edinburgh, UK.
[4]Department of Paleo-climatology and Geomorphology, Faculty of Earth and Life Sciences, Vrije Universiteit Amsterdam, Amsterdam, Netherlands.

Copyright 2010 by the American Geophysical Union.
0883-8305/10/2009PA001857

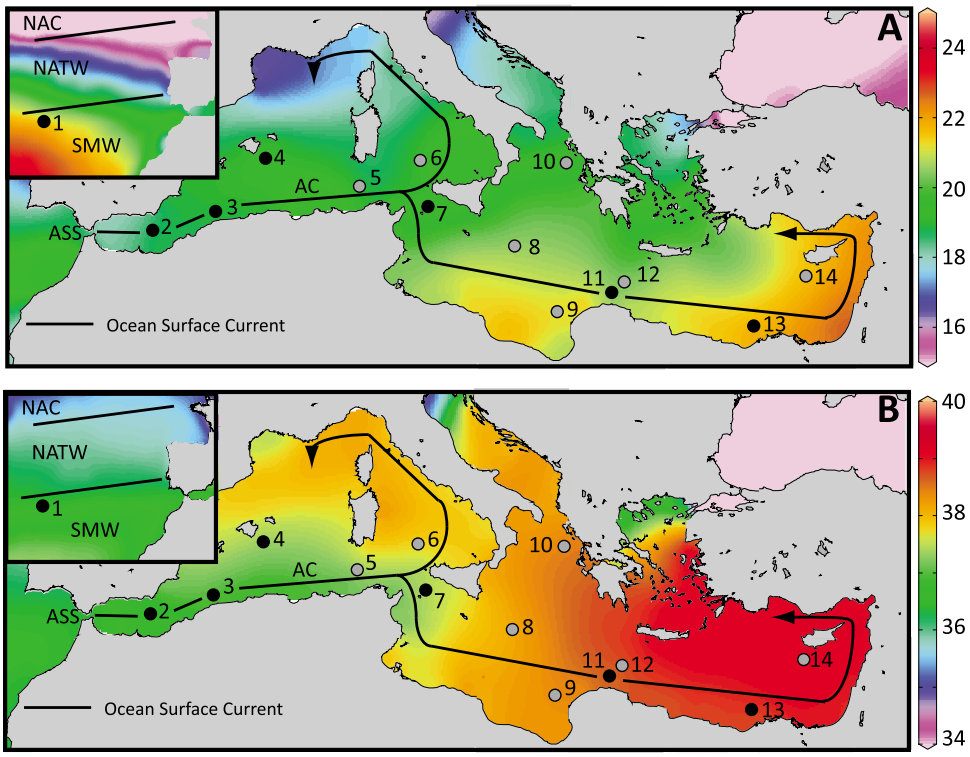

Figure 1. (a) Annual average temperatures of the Mediterranean Sea and North Atlantic in °C. (b) Annual average salinity of the Mediterranean Sea and North Atlantic. ASS, Atlantic Stream System; AC, Algerian Current; NAC, North Atlantic Current; NATW, North Atlantic Tropical Water; SMW, Subtropical Mode Water. Black dots indicate sample locations where enough individual specimens are measured to obtain a reliable measure of seasonality. Grey dots indicate sample locations where not enough samples were measured. The black arrows represent major surface currents. The number at each sample location corresponds to the number of each station in Table 1.

surface temperatures in numerous locations [e.g., *Elderfield and Ganssen*, 2000; *Ganssen and Kroon*, 2000; *Anand et al.*, 2003] and occurs throughout the year in the Mediterranean Sea [*Pujol and Vergnaud-Grazzini*, 1995; *Bárcena et al.*, 2004].

[5] Here we used a new approach aiming at quantifying seasonal temperature changes in marine sediments by combining single-specimen oxygen isotope and Mg/Ca data from planktonic foraminifera, following earlier approaches by *Spero and Williams* [1989], *Billups and Spero* [1996], *Ganssen et al.* [2005] and *Koutavas et al.* [2006]. In order to test the general applicability of our approach, we determined paired δ^{18}O- and Mg/Ca-derived temperature estimates of individual tests of *G. ruber* in a suite of surface sediment samples across the Mediterranean Sea, and then compared the results to the present-day range in sea surface temperatures.

2. Surface Hydrography of the Mediterranean Sea

[6] The Mediterranean Sea is a semienclosed basin, which can be divided into western and eastern basins (Figure 1). The general surface ocean circulation pattern is controlled by Atlantic surface water entering the Alboran Sea via the Strait of Gibraltar as the Atlantic Stream System (ASS) [*Ovchinnikov*, 1966; *Millot*, 1987]. Further eastward the ASS continues as the Algerian Current (AC). The AC splits into two parts, one entering the Tyrrhenian Sea, the other entering the eastern Mediterranean through the Strait of Sicily [*Ovchinnikov*, 1966; *Millot*, 1987]. The AC continues to flow through the Tyrrhenian Sea toward the Gulf of Lions. Further eastward the AC enters the Ionian Sea where it flows mainly eastward toward the Levantine Basin [*Ovchinnikov*, 1966].

[7] Seasonal temperature variation for surface waters (0–50 m) throughout the Mediterranean varies between 14.1°C and 24.8°C, with an annual average around 20°C. Temperatures increase from west to east, as a result of the eastward surface water transport and the warm Mediterranean climate. The seasonal temperature contrasts are similar in the eastern and western Mediterranean being on average 7.3 ± 1°C (Figure 1a and Table 1). Salinity (0–50 m) seasonally varies between 36.8 and 39.3, with an annual average of 38.2 over the entire Mediterranean Basin. The eastward flow of the surface waters, together with excess evaporation in the Mediterranean, causes a gradual increase in salinity from west to east (Figure 1b and Table 1). Seasonal changes

Table 1. Geographical Position, Depth Temperature, and Salinity for All Core Top Samples[a]

Sample	Number	Location	Longitude (°E)	Latitude (°N)	Depth (m)	WOA01 Temperature (°C)	WOA01 Salinity (psu)
T86/11S	1	North Atlantic	−35.57	32.55	2220	20.84 (17.04–23.00)	36.62 (36.40–36.82)
T87/132	2	Alboran Sea	−2.91	35.78	936	17.34 (14.62–20.03)	36.79 (36.62–36.96)
T87/114	3	Algeria	2.59	36.94	1100	17.53 (14.49–20.79	37.05 (36.94–37.15)
M40-4-88-1	4	Balearic Basin	4.60	38.94	1891	17.94 (14.11–22.59)	37.37 (37.27–37.47)
T87/83	5	Tunisia	8.76	37.70	1301	17.61 (14.28–21.27)	37.35 (37.07–37.70)
T87/61	6	Tyrrhenian Sea	11.34	38.25	1246	17.68 (14.12–21.76)	37.60 (37.45–37.81)
T87/49	7	Strait of Sicily	12.12	36.67	1205	18.20 (14.57–22.78)	37.42 (37.22–37.68)
T87/30	8	Ionian Sea	16.42	34.47	1400	19.60 (15.83–24.22)	38.07 (37.88–38.29)
M51-3-562	9	Libya	19.19	32.77	1391	19.90 (16.15–24.40)	38.33 (38.14–38.59)
T87/14	10	Greece	19.92	38.57	1999	17.98 (14.66–21.49)	38.49 (38.41–38.61)
T83/63	11	Libya	22.98	33.12	1093	19.36 (16.05–23.44)	38.63 (38.30–38.95)
M51-3-563	12	Libya	23.50	33.72	1851	19.26 (16.04–22.92)	38.76 (38.51–38.99)
T83/23	13	Nile Delta	29.41	31.88	1465	20.62 (16.51–24.83)	38.88 (38.21–39.11)
M51-3-569	14	Levantine Basin	32.58	33.43	1307	20.48 (16.59–24.25)	39.04 (38.90–39.26)

[a]Temperatures and salinity correspond to the 0–50 m depth average and come from the World Ocean Atlas 2001 (WOA01) database. Values are listed as averages and monthly minima and maxima [*Conkright et al.*, 2002].

in salinity do not vary from east to west, being 0.4 ± 0.2 (Table 1) on average.

[8] Surface water transport in the central North Atlantic is mainly controlled by the northeastward flowing Gulf Stream. Surface water (0–50 m) temperatures at central North Atlantic site T86/11S vary seasonally between 17.0°C and 23.0°C, with an annual average of 20.8°C. Salinity seasonally varies between 36.4 and 36.8 with an annual average of 36.6. On an inter annual time scale variability is probably controlled by branching of the Gulf Stream at 40°N-40°W into the North Atlantic Current (NAC) and the North Atlantic Tropical Water (NATW) [*Hopkins*, 1991]. A second contributor to inter annual variability is the shifting boundary between the NATW and the Subtropical Mode Water (SMW) [*Hopkins*, 1991] (Figure 1).

3. Material and Methods

[9] Core top sediment samples from areas covering a substantial part of the regional oceanographic differences in the Mediterranean Sea and the North Atlantic were used for picking planktonic foraminifera (Figure 1 and Table 1). The T83, T86 and T87 box core samples were retrieved during 3 cruises of the R/V *Tyro* covering all major basins of the Mediterranean Sea and North Atlantic [*Ottens*, 1991; *De Rijk et al.*, 1999; *Ganssen and Kroon*, 2000]. The M40/4, M51/3 and M52/2 core top samples were recovered during 3 cruises of the R/V *Meteor* in the eastern Mediterranean [*Hemleben*, 2002; *Hübscher*, 2002].

[10] A 1–2 cm core top slice from every sediment core was processed for foraminiferal analyses. In order to optimize sieving, samples were put in a sampling cup with distilled water and subsequently shaken for 90 min. Samples were wet-sieved into a >150 μm fraction and dried at 40°C. The dried >150 μm fraction was subsequently sieved into 3 subfractions: 150–250, 250–400 and >600 μm. Specimens of the planktonic foraminiferal species *Globigerinoides ruber* were picked from the 250–400 μm fraction.

[11] The $\delta^{18}O$ values of single specimens of *G. ruber* were measured on a Mat Finnigan 252 gas-source mass spectrometer with an automated Kiel type carbonate preparation line and results were reported relative to the Vienna Pee Dee Belemnite standard (V-PDB). Calibration to the V-PDB was achieved through the NBS-19 standard. The internal reproducibility for $\delta^{18}O$ was ±0.08‰. Estimates of the calcification temperatures based on stable oxygen isotopes were calculated using the temperature equation of *O'Neil et al.* [1969] as refitted by *Shackleton* [1974] (equation (1)).

$$T = 16.9 - 4.38\left(\delta^{18}O_c - \delta^{18}O_w\right) + 0.1\left(\delta^{18}O_c - \delta^{18}O_w\right)^2 \quad (1)$$

The $\delta^{18}O_w$ values were calculated using the salinity–$\delta^{18}O_w$ relationship for the Mediterranean Sea based on the data from *Pierre* [1999] and *Schmidt et al.* [1999] (equation (2)) and North Atlantic [*Ganssen and Kroon*, 2000].

$$\delta^{18}O_w = 0.285S - 9.47 \quad (2)$$

$\delta^{18}O_w$ values were converted from SMOW values to the V-PDB scale with the 0.27‰ correction of *Hut* [1987]. We used annual average salinities for both areas, obtained from the World Ocean Atlas 01 (WOA01) database, since the seasonal timing of calcification is unknown [*Conkright et al.*, 2002]. Using annual average salinity introduced a potential error when calculating seasonal temperatures from individual foraminifera, even though seasonal variations in salinity were small for most sites (Table 1). Consequences of the use of annual average salinity for measured temperature variability will be dealt with in section 5.2.1.

[12] We tested the measured $\delta^{18}O$ distributions for normality with a Shapiro-Wilk test (Table 2). None of the measured distributions significantly deviated from normality ($p < 0.05$) allowing a Gaussian filter to identify outliers. This approach enabled a quantitative comparison of the derived seasonal variation, expressed as 4 standard deviations (4 σ) with the maximum seasonal variation (range) as found in WOA01 database [*Conkright et al.*, 2002]. The whole range of WOA01 database temperatures was used, because temperature values already consisted of averaged monthly temperature data over multiple years and are, therefore, already filtered for outliers [*Conkright et al.*, 2002].

Table 2. Standard Deviations With 95% Confidence Intervals and p Values for the Shapiro-Wilk Test per Sample Location[a]

Sample	Standard Deviation (°C)	Sample Size	Range 95% Confidence Intervals (°C)	Degrees of Freedom	p Value Shapiro-Wilk Test
T86–11S	2.86	26	1.70	25	0.522
T87/132	1.94	16	1.57	15	0.421
T87/114	2.21	15	1.87	14	0.872
M40-4-88-1	2.39	17	1.86	16	0.629
T87/83	3.32	9	4.12	8	0.723
T87/61	2.47	15	2.09	14	0.372
T87/49	2.32	37	1.13	36	0.113
T87/30	2.95	15	2.49	14	0.387
M51-3-562	3.00	16	2.43	15	0.238
T87/14	3.28	8	4.51	7	0.147
T83/63	2.39	19	1.73	18	0.143
M51-3-563	3.42	15	2.89	14	0.960
T83/23	2.84	32	1.50	31	0.263
M51-3-569	3.08	10	3.50	11	0.580
Mediterranean	2.77	224	0.52	223	0.248
T86/11S (Mg/Ca)	3.76	15	3.18	14	0.067
T87/49 (Mg/Ca)	3.80	46	1.63	45	0.748

[a]A $p > 0.05$ indicates that the sample distribution is not significantly deviating from normality.

[13] Subsequently, we calculated 95% confidence limits of our standard deviations to evaluate their accuracy and to establish a clear criterion for a reliable estimate for seasonality, using the χ^2 distribution. Confidence limits may be calculated, since all measured distributions were not significantly deviating from normality. The standard deviation narrowed with increasing number of measurements. These constrains could be expressed as confidence intervals around the measured standard deviation and were calculated with equation (3) [*Bluman*, 2004],

$$\sigma^*\sqrt{(n-1)}/\chi^2_{right} \langle \sigma \rangle \sigma^*\sqrt{(n-1)}/\chi^2_{left} \quad (3)$$

in which σ is the measured standard deviation, **n** is the number of measurements and χ^2_{right} and χ^2_{left} represent the values from the χ^2 distribution at the 95% confidence level. This implies a 95% probability of the standard deviation having a value within this confidence interval. Table 2 shows the 95% range around our calculated standard deviations based on single-specimen analyses. We aimed to measure at least 25 specimens per sample, in order to get a reliable seasonality estimate (4 σ). Standard deviations were only used for reconstructing seasonality if the range in confidence limits was smaller than 2°C. This is a rather large range, due to the limited number of analyses available at each site. Although results appeared robust, large uncertainties are potentially associated with using limited sample sizes.

[14] Samples for trace element analyses were sonically rinsed with MilliQ water 6 times and twice with MeOH for the removal of contaminated sediment following *Barker et al.* [2003]. Trace metal concentrations were measured on one or multiple chambers per individual with laser ablation ICP-MS. Multiple measurements per chamber were not possible, due to the limited test size and thickness of each individual chamber. Foraminifera were ablated with a deep-ultraviolet-wavelength laser (193 nm) using a Lambda Physik excimer laser system with GeoLas 200Q optics. Test carbonate was ablated with a 80 μm beam diameter and a pulse repetition of 5 Hz for approximately 30–60 s with an energy density of 1 J/cm^2. Ablated material was transported on a He gas flow and mixed with Argon. Element to calcium ratios were quantified using ^{24}Mg, ^{26}Mg, ^{27}Al, ^{42}Ca, ^{43}Ca, ^{44}Ca, ^{55}Mn, ^{88}Sr isotopes and their relative natural abundances on a quadrapole ICP-MS instrument (Micromass Platform). Raw counts were converted to elemental concentrations using computer software (Glitter). Elemental ratios were based on averaging the measured concentrations of the 100–300 pulses during each ablation (Figure 2). Calibration is performed against U.S. National Institute of Standards and Technology SRM N610 glass (4 J/cm^2) and an in-house calcite standard GJR (1 J/cm^2) with Ca as an internal standard [*Reichart et al.*, 2003].

[15] Changing the energy density from standard to sample could potentially influence trace metal concentrations measured. Laser ablation analyses, using different energy densities, was therefore compared to solution ICP-OES analyses of the same matrix matched calcite standard (GJR). Values showed no significant offset between results of both techniques and, therefore, changing energy density from standard to sample caused no appreciable offset (Table 3). Measurements were checked for contaminations by evaluating Al and Mn profiles acquired during ablation. Clay particles or postdepositional Mn-rich inorganic coatings, still attached to tests after cleaning, potentially offset the analyses. Both have a higher Mg concentration compared to the test, biasing the Mg measurements. Samples with high Al and Mn concentrations were, therefore, excluded from further evaluation (Figure 3). Measured Mg/Ca ratios were converted to temperature using the calibration of *Anand et al.* [2003] (equation (4)).

$$Mg/Ca = 0.395e^{(0.09T)} \quad (4)$$

This calibration is based on a series of sediment trap samples spanning 6 years, covering multiple seasonal cycles [*Anand et al.*, 2003]. The calibration of *Dekens et al.* [2002],

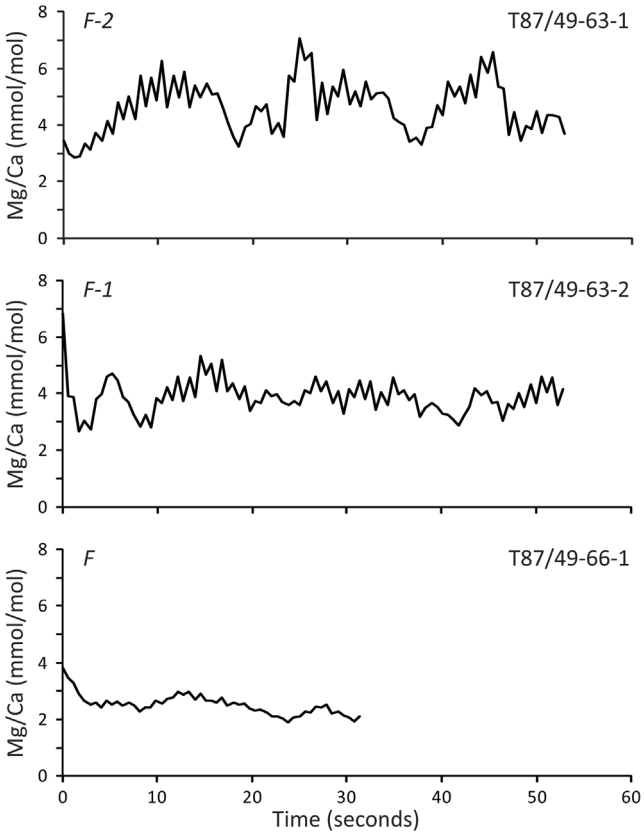

Figure 2. Measured Mg/Ca ratios for three different chambers of *G. ruber* during individual ablations. The Mg/Ca value of each test chamber is determined by averaging the Mg/Ca ratios acquired while ablating the down test. The last chamber (F) has less variability than F-1 and F-2, in line with previous results [*Sadekov et al.*, 2008].

based on core top samples, closely resembled the calibration by *Anand et al.* [2003], whereas the calibration by *Elderfield and Ganssen* [2000] suggested a somewhat higher sensitivity of the foraminiferal Mg/Ca ratio to temperature.

Table 3. Comparison Between Offline Analyses of Discrete Samples Dissolved and Subsequently Measured on ICP-OES and Laser Ablation ICP-MS Analyses[a]

	Mg	Mn	Sr
ICP-OES			
Average	663	99	173
Standard deviation	35	0.40	4.3
Standard deviation (%)	5.2	0.41	2.5
N	3	3	3
LA-ICP-MS			
Average	674	106	184
Standard deviation	61	7.2	15
Standard deviation (%)	9.1	6.9	8.0
N (4 year average)	643	643	643
Ratio	1.016	1.068	1.068

[a]Values are listed in parts per million (ppm).

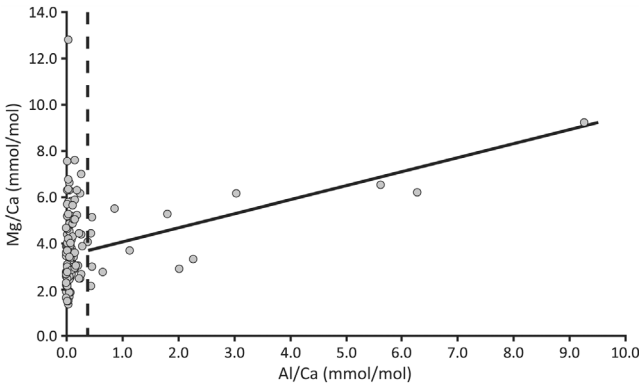

Figure 3. Mg/Ca plotted versus Al/Ca. The black line represents a relation between Al/Ca and Mg/Ca, suggesting a contaminant phase. Subsequently, a cutoff point of 0.4 mmol/mol was used as the maximum acceptable Al/Ca ratio, below which no appreciable effect is noticed. Measurements to the right of the dashed line are therefore excluded from further consideration. Contamination is also recognized when evaluating the laser ablation profile of each individual measurement.

[16] Measured Mg/Ca distributions were also tested for a normal distribution pattern with a Shapiro-Wilk test. Both stations T87/49 and T86/11S were not deviating from normality and results could be fitted with a Gaussian curve. Standard deviations were only used for reconstructing seasonality if the range in the 95% confidence limit was smaller than 2°C, following the same approach as used for the oxygen isotopes.

4. Results

[17] Here we present the combined results from the Mediterranean and Atlantic box cores. For stations T87/83, T87/30, T87/14, M51-3-562, M51-3-563 and M51-3-569 not enough stable oxygen isotope data were available (i.e., confidence intervals larger than 2°C) whereas for station T86/11S not enough Mg/Ca data was obtained. These stations are therefore not discussed individually (Figure 1 and Table 2). The $\delta^{18}O$ data for individual samples display a normal (Gaussian) distribution pattern (Tables 2, 4, and 5 and Figure 4). The observed basin wide range in stable oxygen isotope variability in the Mediterranean Sea is 3.30‰, with a minimum of −0.90‰ (M40-4-88-1) and a maximum of 2.20‰ (M51-3-563). Figure 5 shows the distribution of the calculated $\delta^{18}O$-derived temperatures together with the observed temperatures from the World Ocean Atlas 2001 database [*Conkright et al.*, 2002]. Variation (4 σ) in $\delta^{18}O$-derived temperature for the Mediterranean sample locations is between 7.8°C (T87/132) and 13.7°C (M51-3-563) (Table 4).

[18] The measured distributions for Mg/Ca can be represented by a Gaussian curve (Table 2). A comparison between single-specimen Mg/Ca measurements of Mediterranean site T87/49 and Atlantic site T86/11S, with fitted normal distribution, and the temperature distribution from the WOA01 is

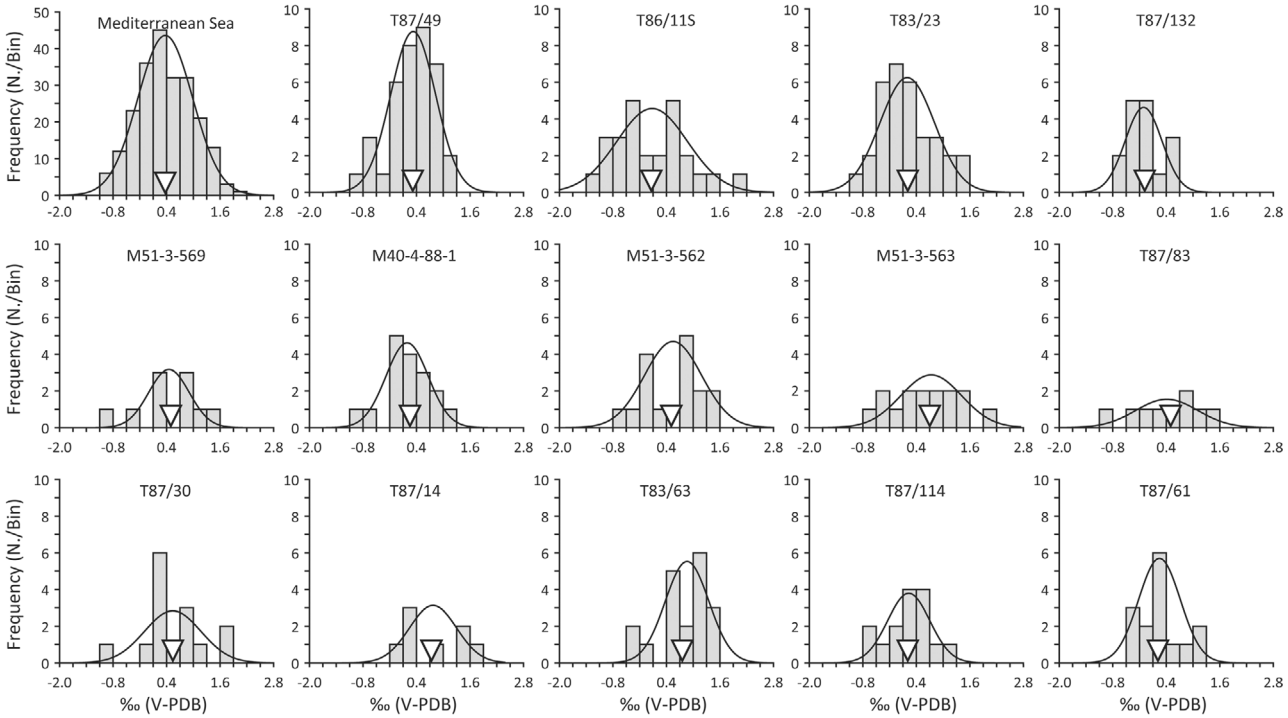

Figure 4. The $\delta^{18}O$ distributions for all sites and the Mediterranean Sea. All distributions are fitted with a Gaussian curve (black line). The frequency axis displays the number of measurements within each bin of the histogram. The open inverted triangle represents average $\delta^{18}O$.

shown in Figure 6. The variation (4 σ) in Mg/Ca data from individual specimen of cores T87/49 and T86/11S is 3.87 mmol/mol (11.3°C) and 3.63 mmol/mol (10.0°C), respectively (Table 6). The variability in Mg/Ca data (1 σ) between individual test chambers for site T86/11S alone ranges between 0.03 and 4.22 mmol/mol.

5. Discussion

5.1. Seasonal Changes in Temperature

5.1.1. Boundary Conditions for Reconstructing Seasonality

[19] Within a specific area of the ocean, the potential of a particular proxy to reconstruct seasonality will depend on how accurately it reflects the seasonal variability in water properties through time. For this study we have selected the planktonic foraminiferal species *G. ruber* because it reproduces at roughly constant levels throughout the year in the Mediterranean Sea and the Atlantic Ocean [*Pujol and Vergnaud-Grazzini*, 1995; *Bárcena et al.*, 2004; *Ottens*, 1991]. The variability in the chemical/physical properties at the sea surface throughout the year should, therefore, be recorded in specimens of *G. ruber* taken from the underlying sediment. The data generated in this study tests this assumption by separately evaluating the average $\delta^{18}O$- and Mg/Ca-derived temperature estimates for each site. When comparing observed annual average temperatures with estimates thereof based on $\delta^{18}O$ and Mg/Ca data, the respective data sets reasonably match each other (Figures 4, 5, and 6). Furthermore, observed differences between average $\delta^{18}O$- or Mg/Ca-derived temperatures, and annual WOA01 temperatures are tested for significance using an independent t-test (Table 7). None of the $\delta^{18}O$-derived averages fail the null hypothesis, supporting that $\delta^{18}O$ values for *G. ruber* are recording annual average sea surface temperatures. Mg/Ca-derived temperatures do, however, not accurately match the annual average temperature (Figure 6 and Table 7). This might be related mainly to two causes. First, Mg/Ca-temperature calibrations are species specific and vary with regional oceanographic settings. Second, Mg/Ca values in the current study are derived from point measurements using laser ablation ICP-MS, while published Mg/Ca-temperature calibrations are based on Mg/Ca data from whole foraminiferal test [*Elderfield and Ganssen*, 2000; *Dekens et al.*, 2002; *Anand et al.*, 2003]. This is potentially causing an offset between Mg/Ca-derived and annual temperatures, because of the more rigorous cleaning techniques used in whole foraminiferal test analyses, which preferentially removes Mg-rich carbonate phases, lowering the overall concentration [*Barker et al.*, 2003].

[20] Another factor impinging on seasonality reconstructions relates to migration of foraminifera through the water column during their life cycle. The effects of changes in depth habitat can be assessed by documenting the $\delta^{13}C$ and $\delta^{18}O$ values of individual foraminifera [*Spero and Williams*, 1988, 1989]. The $\delta^{13}C$ values of Mediterranean Sea surface waters (0–50 m) are rather constant over short time scales [*Pierre*,

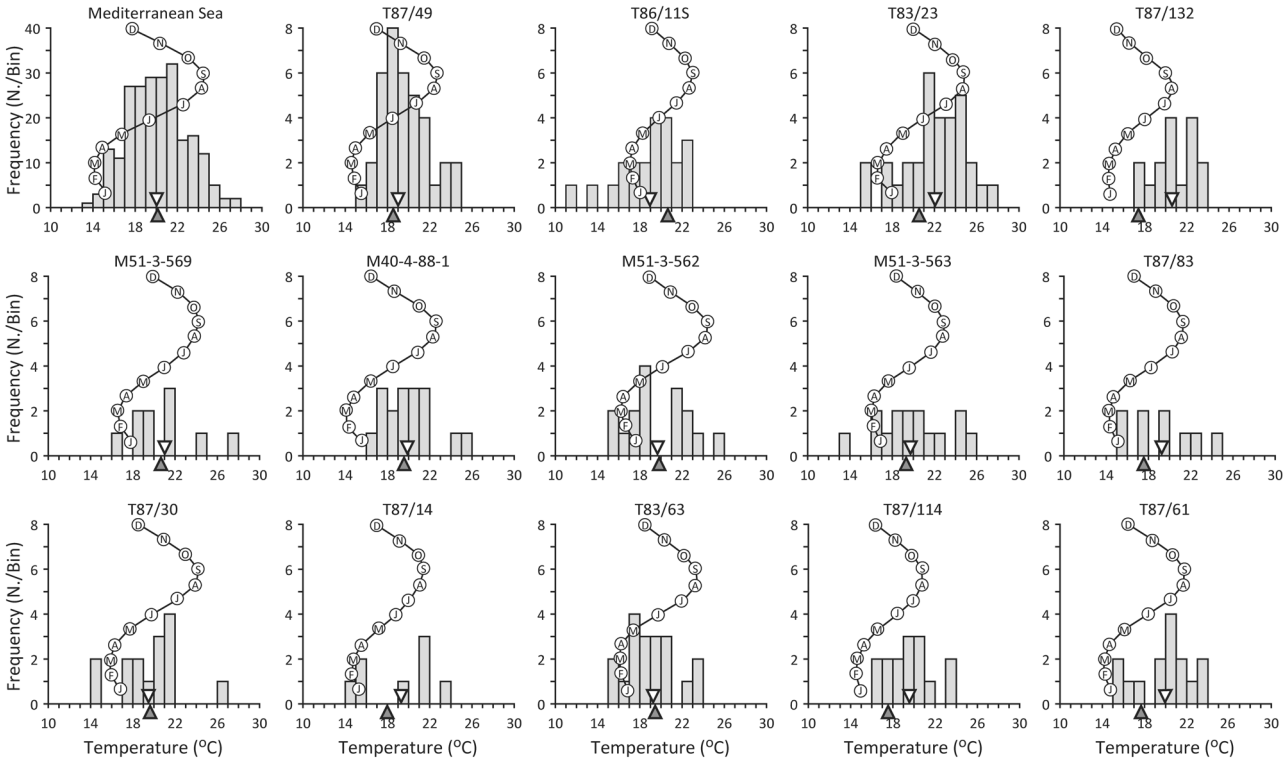

Figure 5. The δ^{18}O-temperature distributions for all sites and Mediterranean Sea water. Calculated temperatures are compared with observed sea surface temperatures (0–50 m) per month from the WOA01 Database [*Conkright et al.*, 2002]. The frequency axis displays the number of measurements in each bin of the histogram. The open inverted triangle represents average δ^{18}O-derived temperature; the grey triangle represents average WOA01-derived temperature.

1999]. Variability in δ^{13}C from foraminifera living within the upper euphotic zone is, therefore, mainly caused by changes in symbiont activity [*Spero and Williams*, 1988, 1989; *Spero*, 1992; *Spero and Lea*, 1993]. Symbiont activity, in turn, is controlled by light intensity in the water column, which is a function of water depth. High light levels correspond to shallow water conditions with enriched δ^{13}C values, while low light conditions correspond to deeper depth habitats and subsequent depleted δ^{13}C values [*Spero and Williams*, 1988, 1989]. Variations in settling depth also affect δ^{18}O values recorded in foraminifera with increasing values generally reflecting deeper habits. If variability in δ^{18}O caused by depth migrations would play a significant role in our calibration, we expect a negative correlation between decreasing δ^{13}C values and rising δ^{18}O values for individual foraminifera as shown by *Spero and Williams* [1988, 1989]. For all but one station (station T87/114), the *r* values for the δ^{18}O–δ^{13}C correlations and the respective significance levels (Tables 8 and 9) show no such correlation. Hence, this finding suggests that our seasonality reconstruction should be largely unaffected by variations in settling depth of *G. ruber* used in this study. Data from station T87/114 have not been used for our seasonality reconstruction.

[21] Additional parameters potentially interfering with our seasonality calibration are variations in sedimentation rates and bioturbation. A low sedimentation rate implies that a

Table 4. Measured and Observed δ^{18}O Seasonality Expressed as 4 σ[a]

Sample	4 σ δ^{18}O (°C)	Range Temperature (°C)	4 σ Salinity (°C)	4 σ [CO_3^{2-}] (°C)
T86–11S	8.50	5.97	0.57	0.21
T87/132	7.76	5.41	0.48	0.16
T87/114	8.84	6.31	0.33	0.18
M40-4-88-1	9.56	8.49	0.30	0.19
T87/83	13.28	6.99	0.89	0.30
T87/61	9.88	7.64	0.47	0.28
T87/49	9.28	8.20	0.71	0.32
T87/30	11.80	8.39	0.61	0.34
M51-3-562	12.00	8.25	0.74	0.43
T87/14	13.12	6.83	0.28	0.22
T83/63	9.56	7.39	1.03	0.47
M51-3-563	13.68	6.88	0.78	0.51
T83/23	11.36	8.32	1.11	1.60
M51-3-569	12.32	7.66	0.55	1.63
Mediterranean	11.08	10.72	0.43	0.94

[a]The δ^{18}O variation (4 σ) for site T86/11S excludes two cold outliers. Salinity and temperature values are from the WOA01 database [*Conkright et al.*, 2002]. [CO_3^{2-}] values are calculated using TCO_2 and alkalinity database values and the CO_2SYS program [*Lewis and Wallace*, 1998; *Goyet et al.*, 2000].

Table 5. *G. ruber* δ^{18}O Values[a]

Sample	δ^{18}O (VPDB)	Sample	δ^{18}O (VPDB)	Sample	δ^{18}O (VPDB)	Sample	δ^{18}O (VPDB)	Sample	δ^{18}O (VPDB)	Sample	δ^{18}O (VPDB)
T86/11S-4	0.43	T87/49	0.57	T83/23	−0.33	M40-4-88-1	−0.06	M51-3-563	1.05	T83/63	0.48
T86/11S	−0.42	T87/49	0.21	T83/23	0.38	M40-4-88-1	0.77	T87/83	0.87	T83/63	−0.23
T86/11S	1.11	T87/49	0.85	T83/23	−0.39	M40-4-88-1	1.06	T87/83	0.75	T83/63	1.09
T86/11S-6	2.12	T87/49-7	0.83	T83/23	0.34	M40-4-88-1	0.88	T87/83	−0.85	T83/63	1.50
T86/11S-10	0.38	T87/49-9	−0.03	T83/23	0.00	M40-4-88-1	0.60	T87/83	−0.19	T83/63	1.52
T86/11S-11	−0.98	T87/49-15	−0.83	T83/23	−0.66	M40-4-88-1	0.39	T87/83	0.33	T83/63	1.08
T86/11S-13	0.51	T87/49-17	0.57	T83/23	−0.18	M40-4-88-1	0.69	T87/83	0.40	T83/63	0.63
T86/11S-16	0.80	T87/49-26	−0.64	T83/23	−0.56	M40-4-88-1	0.06	T87/83	−0.24	T83/63	1.01
T86/11S	−0.31	T87/49-18	−0.20	T83/23	−0.40	M40-4-88-1	−0.90	T87/83	1.34	T83/63	0.94
T86/11S	−0.22	T87/49-48	0.73	T83/23	0.23	M40-4-88-1	0.39	T87/83	1.30	T83/63	1.12
T86/11S	0.50	T87/49-50	0.35	T83/23	0.16	M40-4-88-1	−0.12	T87/30	0.16	T87/114	0.29
T86/11S	0.61	T87/49-51	0.02	T87/132	−0.48	M40-4-88-1	−0.70	T87/30	0.91	T87/114	0.66
T86/11S	0.06	T87/49-57	0.82	T87/132	0.07	M51-3-562	0.88	T87/30	0.06	T87/114	−0.25
T86/11S	1.54	T87/49-58	0.99	T87/132	−0.48	M51-3-562	0.76	T87/30	0.74	T87/114	0.10
T86/11S	−0.72	T87/49-59	0.51	T87/132	0.04	M51-3-562	1.47	T87/30	0.14	T87/114	0.24
T86/11S	−0.60	T87/49-60	0.84	T87/132	−0.05	M51-3-562	−0.69	T87/30	1.72	T87/114	0.24
T86/11S	0.18	T87/49-63	−0.75	T87/132	−0.43	M51-3-562	0.90	T87/30	1.65	T87/114	1.01
T86/11S-20	−0.38	T87/49-66	0.65	T87/132	−0.34	M51-3-562	0.95	T87/30	0.30	T87/114	0.00
T86/11S-21	−0.28	T87/49-47	0.28	T87/132	0.00	M51-3-562	1.47	T87/30	−0.88	T87/114	0.48
T86/11S	0.00	T87/49-52	1.16	T87/132	−0.73	M51-3-562	0.08	T87/30	0.57	T87/114	−0.01
T86/11S	−1.21	T87/49-55	0.34	T87/132	0.62	M51-3-562	−0.25	T87/30	1.07	T87/114	0.43
T86/11S	0.55	T83/23	0.74	T87/132	−0.42	M51-3-562	1.28	T87/30	0.24	T87/114	0.83
T86/11S	−0.52	T83/23	0.30	T87/132	−0.06	M51-3-562	1.08	T87/30	0.35	T87/114	−0.71
T86/11S	0.74	T83/23	1.56	T87/132	0.42	M51-3-562	0.08	T87/30	0.84	T87/114	−0.58
T86/11S	−0.89	T83/23	0.06	T87/132	0.24	M51-3-562	0.10	T87/30	0.18	T87/114	0.69
T86/11S	−0.93	T83/23	−0.48	T87/132	0.56	M51-3-562	−0.08	T87/14	0.12	T87/61	0.28
T87/49-1	0.17	T83/23	0.73	T87/132	−0.71	M51-3-562	−0.06	T87/14	0.10	T87/61	1.02
T87/49-10	1.04	T83/23	0.09	M51-3-569	0.33	M51-3-562	0.82	T87/14	−0.12	T87/61	−0.40
T87/49-14	−0.42	T83/23	1.16	M51-3-569	−0.87	M51-3-563	−0.26	T87/14	0.30	T87/61	0.41
T87/49	−0.09	T83/23	−0.20	M51-3-569	0.93	M51-3-563	0.98	T87/14	0.70	T87/61	−0.09
T87/49	0.62	T83/23	1.55	M51-3-569	1.01	M51-3-563	−0.39	T87/14	1.72	T87/61	0.85
T87/49	0.60	T83/23	1.26	M51-3-569	0.28	M51-3-563	2.20	T87/14	1.47	T87/61	0.24
T87/49	0.06	T83/23	0.44	M51-3-569	0.81	M51-3-563	−0.52	T87/14	1.47	T87/61	−0.24
T87/49	0.12	T83/23	−0.32	M51-3-569	−0.24	M51-3-563	0.30	T83/63	0.59	T87/61	0.27
T87/49	0.57	T83/23	0.86	M51-3-569	0.81	M51-3-563	0.64	T83/63	0.56	T87/61	0.03
T87/49	0.34	T83/23	0.53	M51-3-569	0.32	M51-3-563	1.19	T83/63	0.72	T87/61	0.18
T87/49	−0.06	T83/23	0.40	M51-3-569	1.43	M51-3-563	0.45	T83/63	1.08	T87/61	1.22
T87/49	0.37	T83/23	0.33	M40-4-88-1	0.07	M51-3-563	0.40	T83/63	0.44	T87/61	0.29
T87/49	0.86	T83/23	−0.03	M40-4-88-1	0.29	M51-3-563	0.08	T83/63	1.36	T87/61	0.11
T87/49	−0.54	T83/23	−0.88	M40-4-88-1	−0.09	M51-3-563	0.72	T83/63	−0.25	T87/61	−0.46
T87/49	0.44	T83/23	−0.26	M40-4-88-1	0.52	M51-3-563	1.41	T83/63	−0.07		
T87/49	0.67	T83/23	−0.16	M40-4-88-1	0.14	M51-3-563	1.50	T83/63	1.01		

[a]Samples measured for paired δ^{18}O-Mg/Ca analyses are listed with an additional number, matching the sample name from Table 6.

larger time interval is sampled, potentially enhancing variability within the sample. Subsequently, bioturbation increases the time interval captured in an individual sample, which also enhances the variability present in the sample. If we use the sedimentation rates at nearby locations of 10–30 cm/kyr [*Rupke et al.*, 1974, and references therein; *Tadjiki and Erten*, 1994; *Rutten et al.*, 2000] as a guideline, the core top samples used in this study encompass 70–200 years. Lower sedimentation rates would result in a longer time period covered in individual samples. Climate variability within the Mediterranean region for the past 200 years encompasses the Little Ice Age [*deMenocal et al.*, 2000; *Schilman et al.*, 2001], potentially increasing the interannual variability in our data set. The good fit between δ^{18}O-derived annual average and database observed annual average temperatures (Figure 5), however, suggests that interannual variability as a result of low sedimentation rates and bioturbation potentially plays a minor to moderate role in the current calibration.

5.1.2. Reconstructing Seasonality

[22] The previous lines of argument support the notion that not only annual average temperatures can be reconstructed using foraminiferal δ^{18}O and Mg/Ca data. The variability as seen in our δ^{18}O and Mg/Ca data set, measured on single-specimen foraminifera, should predominantly reflect seasonal variations in sea surface temperature. We, therefore, made a direct comparison between the temperature variation (4 σ) deduced from the δ^{18}O data and the observed temperature range of the WOA01 (Max-Min), using only samples with a range in confidence limits of the standard deviation smaller than 2°C (Table 2 and Figure 7). The linear correlation between δ^{18}O-derived temperature variation and WOA01 temperature range is remarkably good (R^2 = 0.70) with a slope of 1.14. We note that the regression line does not go through the origin, which is indicative of other factors influencing this relation as well. This suggests that δ^{18}O measurements on individual foraminifera can be used to

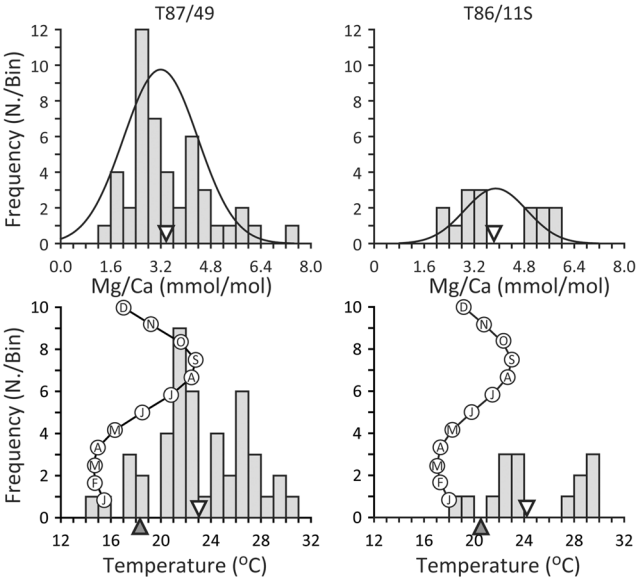

Figure 6. Mg/Ca and Mg/Ca-derived temperature distributions for sites T87/49 and T86/11S. Mg/Ca distributions are fitted with a Gaussian curve (top). The frequency axis displays the number of measurements in each bin of the histogram. Mg/Ca-derived temperatures are compared with observed sea surface temperatures (0–50 m) per month from the WOA01 Database [*Conkright et al.*, 2002]. The open inverted triangle represents average Mg/Ca-derived temperature; the grey triangle represents average WOA01-derived temperature.

reconstruct the seasonal temperature contrast, although other causes for $\delta^{18}O$ variability must be kept in mind.

5.2. Additional Causes for $\delta^{18}O$ and Mg/Ca Variability

[23] In addition to seasonal changes in sea surface temperature other factors may influence shell chemistry and stable isotopic composition such as (1) salinity, (2) carbonate chemistry ($[CO_3^{2-}]$), (3) symbiont activity, (4) ontogenetic effects and (5) natural variability caused by unknown factors [*Spero et al.*, 1997; *Schiebel and Hemleben*, 2005]. We evaluate these parameters, calculating their potential impact on the $\delta^{18}O$-Mg/Ca variability and, therefore, the recording of seasonality.

5.2.1. Salinity

[24] Local fluctuations in the precipitation/evaporation balance can alter the S: $\delta^{18}O_w$ relation [*Rohling*, 1999]. In the Mediterranean Sea, however, the S:$\delta^{18}0_w$ relation is relatively constant on a monthly to seasonal time scale limiting the bias in our data due to variations in the evaporation/precipitation balance [*Rohling and Bigg*, 1998]. Also, the use of average annual salinity values instead of actual salinity values during calcification adds uncertainty to the $\delta^{18}O_c$-derived temperature. A seasonal offset of 0.1 in salinity would lead to an uncertainty of 0.12°C in $\delta^{18}O$-derived temperature, when using equations (1) and (2) (Table 4), based on the WOA1 data. The effect of salinity is directly opposing the temperature effect on $\delta^{18}O_c$. Warm dry summers are concurring with high salinities in the Mediterranean, while low salinities are occurring during the relatively cold and wet winter. Warm summer temperatures result in lower $\delta^{18}O_c$ values, while the covarying high summer salinities cause higher $\delta^{18}O_c$ values and vice versa in the winter. The combined effect due to interannual variations in summer and winter salinities through time, adds up to standard deviations in salinity between 0.06 and 0.24 psu, implying a 2–11% uncertainty in $\delta^{18}O$-derived temperature.

[25] Seasonal variations in salinity can also interfere with Mg/Ca as a temperature proxy. A change of 0.1 psu in salinity translates into an increase of 0.06°C in Mg/Ca based temperatures [*Kisakürek et al.*, 2008], independent of changes in carbonate chemistry [*Dueñas-Bohórquez et al.*, 2009]. Fluctuations in salinity could thus explain 1.8% (T86/11S) and 2.2% (T87/49) of the measured Mg/Ca-derived temperature standard deviations.

5.2.2. Carbonate Chemistry

[26] Changes in the carbonate chemistry of the ambient seawater ($[CO_3^{2-}]$) potentially influence foraminiferal $\delta^{18}O$ and Mg/Ca values [*Spero et al.*, 1997; *Russell et al.*, 2004]. The concentration of CO_3^{2-} in seawater influences the oxygen isotope signal of *G. ruber* with −0.0022‰ per μmol/kg change [*Russell and Spero*, 2000]. An increase of 10 μmol/kg in carbonate ion concentration leads to an increase of 0.09°C for $\delta^{18}O$. Calculated standard deviations in $[CO_3^{2-}]$ and its influence on $\delta^{18}O$-derived temperatures for all sites are in Table 4. Changes in carbonate ion concentration could explain 2–14% of the measured standard deviation in $\delta^{18}O$-derived temperatures.

[27] The same calculations were made to evaluate the carbonate ion effect on the Mg/Ca-derived temperatures. The Mg/Ca concentration in symbiont bearing planktonic species *Orbulina universa* changes with −0.021 μmol/kg per unit change in $[CO_3^{2-}]$ [*Russell et al.*, 2004]. Assuming this slope to be the same order of magnitude for *G. ruber*, since both species are symbiont bearing and live in a similar habitat, an increase of 10 μmol/kg in carbonate ion concentration leads to a decrease of 0.27°C for Mg/Ca based temperatures. Hence, 4.2% (T86/11S) and 6.5% (T87/49) of the standard deviation of Mg/Ca-derived temperatures could be attributed to a carbonate ion effect.

5.2.3. Symbiont Activity

[28] A major impact of symbiont activity on foraminiferal $\delta^{13}C$ values has been demonstrated [*Spero and Williams*, 1988, 1989; *Spero*, 1992; *Spero and Lea*, 1993]. Impact of symbiont activity on foraminiferal $\delta^{18}O$ is, however, much smaller [*Spero et al.*, 1997]. Hence a linear relationship between the temperatures during the main period of reproduction of *G. ruber* and the overall $\delta^{18}O$ temperature at each site is still expected. Except for sites T87/132 (Alboran Sea) and T83/23 (Nile Delta) such a relationship indeed exists. With regard to the Alboran Sea, this area of the Mediterranean Sea is largely influenced by the Atlantic Ocean, leading to a more seasonal reproduction pattern of *G. ruber*. Fluctuations in Nile runoff reflect seasonal changes in precipitation, which has a large influence on the $\delta^{18}O$-salinity relation, explaining the aberrant data at station T83/23. Overall, the correlation between the general $\delta^{18}O$-derived temperature and the temperature during peak reproduction periods of

Table 6. Mg/Ca Values of *G. ruber*[a]

Sample	Chamber	Mg/Ca (mmol/mol)	Sample	Chamber	Mg/Ca (mmol/mol)	Sample	Chamber	Mg/Ca (mmol/mol)
T86/11S-4-01	F-1	5.28 ± 0.40	T86/11S-20-01	F-2	6.28 ± 0.67	T87/49-68-1	F-2	2.56 ± 0.29
T86/11S-4-02	F-4	6.6 ± 0.50	T86/11S-20-02	F-1	5.17 ± 0.56	T87/49-69-1	F-2	2.77 ± 0.32
T86/11S-4-03	F	2.53 ± 0.19	T86/11S-20-03	F	3.67 ± 0.40	T87/49-70-1	F-2	2.21 ± 0.25
T86/11S-4-04	F-2	6.75 ± 0.51	T86/11S-21-01	F-1	3.37 ± 0.39	T87/49-70-2	F-1	2.13 ± 0.25
T86/11S-6-01	F-2	3.61 ± 0.28	T86/11S-21-02	F-3	2.89 ± 0.34	T87/49-71-1	F-2	2.47 ± 0.29
T86/11S-6-02	F	3.04 ± 0.23	T86/11S-21-03	F	1.87 ± 0.22	T87/49-72-1	F-2	3.06 ± 0.36
T86/11S-7-01	F-1	3.75 ± 0.29	T86/11S-22-01	F-2	7.55 ± 0.87	T87/49-36-1	F-1	2.28 ± 0.11
T86/11S-7-03	F	2.67 ± 0.21	T86/11S-22-02	F-1	5.74 ± 0.67	T87/49-36-2	F-2	1.50 ± 0.08
T86/11S-9-01	F-1	3.22 ± 0.26	T86/11S-22-03	F	3.81 ± 0.45	T87/49-1-1	F-1	2.76 ± 0.14
T86/11S-9-02	F-2	3.67 ± 0.29	T87/49-47-1	F-2	4.36 ± 0.37	T87/49-2-1	F-1	5.12 ± 0.25
T86/11S-9-03	F	2.46 ± 0.20	T87/49-47-2	F-1	4.52 ± 0.39	T87/49-2-2	F-2	4.37 ± 0.22
T86/11S-10-01	F-2	5.14 ± 0.42	T87/49-48-1	F-1	2.95 ± 0.25	T87/49-5-1	F-1	3.60 ± 0.19
T86/11S-10-02	F-1	6.28 ± 0.51	T87/49-50-1	F-2	1.85 ± 0.16	T87/49-6-1	F-1	2.68 ± 0.14
T86/11S-11-01	F-2	5.81 ± 0.50	T87/49-51-1	F-2	1.35 ± 0.12	T87/49-7-1	F-2	3.35 ± 0.18
T86/11S-11-02	F-1	5.17 ± 0,45	T87/49-51-2	F-2	1.47 ± 0.13	T87/49-8-1	F-1	7.60 ± 0.41
T86/11S-12-01	F-1	3.15 ± 0.27	T87/49-52-1	F-1	1.63 ± 0.15	T87/49-9-1	F-1	2.48 ± 0.14
T86/11S-12-03	F	2.64 ± 0.23	T87/49-53-1	F-1	4.24 ± 0.39	T87/49-10-1	F-1	2.93 ± 0.16
T86/11S-13-01	F-3	3.22 ± 0.28	T87/49-54-1	F-1	2.74 ± 0.25	T87/49-12-1	F-1	2.99 ± 0.17
T86/11S-13-02	F-1	4.08 ± 0.36	T87/49-55-1	F-2	3.46 ± 0.32	T87/49-13-1	F-2	2.65 ± 0.15
T86/11S-13-03	F-2	3.00 ± 0.27	T87/49-57-1	F-2	3.02 ± 0.29	T87/49-14-1	F-1	4.64 ± 0.27
T86/11S-13-04	F	1.58 ± 0.15	T87/49-57-2	F-1	3.93 ± 0.38	T87/49-15-1	F-2	2.73 ± 0.16
T86/11S-14-01	F-1	3.1 ± 0.29	T87/49-58-1	F-2	2.69 ± 0.26	T87/49-16-1	F-1	6.33 ± 0.38
T86/11S-14-02	F	3.36 ± 0.31	T87/49-59-1	F-1	4.13 ± 0.40	T87/49-17-1	F-2	2.99 ± 0.18
T86/11S-15-01	F-1	2.79 ± 0.26	T87/49-60-1	F-2	4.00 ± 0.41	T87/49-18-1	F-1	1.89 ± 0.12
T86/11S-15-02	F-2	2.23 ± 0.21	T87/49-61-1	F-2	2.13 ± 0.22	T87/49-19-2	F-1	4.18 ± 0.27
T86/11S-15-03	F	2.07 ± 0.20	T87/49-62-1	F-2	5.24 ± 0.54	T87/49-23-1	F-2	3.84 ± 0.25
T86/11S-16-01	F-2	4.80 ± 0.46	T87/49-63-1	F-2	4.62 ± 0.48	T87/49-24-1	F-1	2.85 ± 0.20
T86/11S-16-02	F-1	4.83 ± 0.46	T87/49-63-2	F-1	3.87 ± 0.41	T87/49-26-1	F-2	3.67 ± 0.26
T86/11S-17-01	F-1	2.75 ± 0.27	T87/49-64-1	F-2	5.88 ± 0.64	T87/49-27-1	F-1	2.73 ± 0.20
T86/11S-17-02	F-2	1.89 ± 0.19	T87/49-65-1	F-2	4.27 ± 0.47	T87/49-29-1	F-1	4.86 ± 0.35
T86/11S-17-03	F	1.67 ± 0.17	T87/49-66-1	F	2.55 ± 0.29	T87/49-30-1	F-1	5.67 ± 0.42
T86/11S-17-04	F-3	2.41 ± 0.25	T87/49-67-1	F-2	3.06 ± 0.34			

[a]Values are listed with one standard deviation.

G. ruber supports the view that the effect of symbiont activity on oxygen isotopes is minor.

[29] With regard to additional effects of symbiont activity on the Mg/Ca ratios in planktonic foraminifera, recent studies have reported large variations between individual foraminiferal tests [*Lea et al.*, 1999] as well as within individual tests [*Sadekov et al.*, 2008]. Alternating layers of high and low Mg concentrations within the foraminiferal chambers of *G. ruber* found off West Australia for example suggested that the changes in Mg/Ca could be connected to symbiont activity [*Sadekov et al.*, 2008]. Observations of the laser ablation Mg/Ca signal over single test chambers used in the present study revealed a similar layering of high and low Mg calcite (Figure 2). However, similar large variations in Mg/Ca are also found in symbiont barren species *Globigerina bulloides, Globorotalia inflata* and *Globorotalia truncatulinoides* [*Anand and Elderfield*, 2005; *Hathorne et al.*, 2009], suggesting symbiont activity is only playing a minor role in Mg/Ca variability.

5.2.4. Ontogenetic Effects

[30] Changes in growth rate related to different life stages of a foraminifer, hence size, have an important effect on the stable isotope composition of their shell [*Kroon and Darling*, 1995; *Spero and Lea*, 1996; *Bijma et al.*, 1998]. Changes in growth rate related to different life stages of a foraminifer, hence size, have an important effect on the stable isotope composition of their shell [*Kroon and Darling*, 1995; *Spero*

Table 7. Independently Calculated t Statistic and Its Significance When Comparing Average δ^{18}O- and Mg/Ca-Derived Temperatures to Annual Temperatures Reported in the WOA01 Database[a]

Sample	t Statistic	DF	Significance
T86/11S	−0.813	32	0.42
T87/132	1.879	17	0.077
T87/114	0.490	25	0.63
M40-88-1	1.890	27	0.070
T87/83	1.159	19	0.26
T87/61	1.625	25	0.12
T87/49	1.659	47	0.10
T87/30	−0.105	25	0.92
M51-3-562	−0.021	25	0.98
T87/14	0.937	18	0.36
T87/63	−0.219	29	0.83
M51-3-563	0.506	25	0.62
T83/23	0.464	42	0.65
M51-3-569	0.418	20	0.68
Mediterranean	−0.492	234	0.62
T86/11S (Mg/Ca)	1.990	18	0.072
T87/49 (Mg/Ca)	4.114	56	0.009

[a]None of the δ^{18}O-derived t statistics are significant ($p < 0.05$), indicating that *G. ruber* captures the annual temperature at each sample location. Calculated t statistics for Mg/Ca-derived temperatures are (almost) significant, indicating that the Mg/Ca of *G. ruber* is not representing annual temperatures at both sample locations.

Table 8. *G. ruber* δ^{13}C Values[a]

Sample	δ^{13}C (VPDB)	Sample	δ^{13}C (VPDB)	Sample	δ^{13}C (VPDB)	Sample	δ^{13}C (VPDB)	Sample	δ^{13}C (VPDB)	Sample	δ^{13}C (VPDB)
T86/11S-4	0.88	T87/49	1.62	T83/23	1.50	M40-4-88-1	1.34	M51-3-563	0.07	T83/63	1.89
T86/11S	1.34	T87/49	0.90	T83/23	1.45	M40-4-88-1	1.20	T87/83	1.00	T83/63	1.65
T86/11S	0.49	T87/49	1.00	T83/23	1.27	M40-4-88-1	0.67	T87/83	0.55	T83/63	1.91
T86/11S-6	0.64	T87/49-7	0.98	T83/23	1.00	M40-4-88-1	0.85	T87/83	1.28	T83/63	0.98
T86/11S-10	0.26	T87/49-9	1.42	T83/23	0.87	M40-4-88-1	1.27	T87/83	0.64	T83/63	1.51
T86/11S-11	−0.02	T87/49-15	0.98	T83/23	0.65	M40-4-88-1	1.66	T87/83	1.91	T83/63	1.81
T86/11S-13	0.14	T87/49-17	0.80	T83/23	0.67	M40-4-88-1	1.28	T87/83	1.65	T83/63	1.36
T86/11S-16	0.15	T87/49-26	0.79	T83/23	0.80	M40-4-88-1	1.38	T87/83	1.31	T83/63	1.93
T86/11S	1.13	T87/49-18	1.29	T83/23	1.39	M40-4-88-1	1.69	T87/83	0.28	T83/63	1.16
T86/11S	0.80	T87/49-48	0.53	T83/23	1.09	M40-4-88-1	1.05	T87/83	1.38	T83/63	1.89
T86/11S	0.60	T87/49-50	1.21	T83/23	1.43	M40-4-88-1	1.22	T87/30	0.61	T87/114	1.25
T86/11S	1.14	T87/49-51	0.41	T87/132	1.63	M40-4-88-1	1.42	T87/30	1.43	T87/114	1.29
T86/11S	0.72	T87/49-57	1.27	T87/132	0.93	M51-3-562	0.99	T87/30	0.65	T87/114	1.48
T86/11S	0.47	T87/49-58	0.82	T87/132	1.06	M51-3-562	1.46	T87/30	0.63	T87/114	1.52
T86/11S	0.01	T87/49-59	1.60	T87/132	1.19	M51-3-562	1.35	T87/30	1.33	T87/114	1.51
T86/11S	0.48	T87/49-60	0.72	T87/132	0.72	M51-3-562	1.03	T87/30	2.33	T87/114	2.04
T86/11S	0.57	T87/49-63	1.47	T87/132	1.57	M51-3-562	0.88	T87/30	2.16	T87/114	0.71
T86/11S-20	0.86	T87/49-66	1.23	T87/132	0.43	M51-3-562	0.82	T87/30	1.21	T87/114	1.30
T86/11S-21	0.59	T87/49-47	0.00	T87/132	0.23	M51-3-562	2.20	T87/30	2.47	T87/114	1.22
T86/11S	0.65	T87/49-52	0.51	T87/132	1.49	M51-3-562	1.08	T87/30	1.03	T87/114	1.61
T86/11S	−0.85	T87/49-55	0.19	T87/132	1.16	M51-3-562	0.69	T87/30	1.97	T87/114	1.49
T86/11S	0.61	T83/23	1.84	T87/132	1.37	M51-3-562	2.10	T87/30	1.49	T87/114	0.99
T86/11S	0.53	T83/23	1.21	T87/132	1.57	M51-3-562	1.71	T87/30	1.45	T87/114	1.29
T86/11S	0.95	T83/23	1.72	T87/132	0.75	M51-3-562	1.03	T87/30	1.17	T87/114	1.56
T86/11S	0.88	T83/23	0.77	T87/132	1.09	M51-3-562	1.13	T87/30	0.72	T87/114	0.51
T86/11S	1.67	T83/23	1.12	T87/132	0.84	M51-3-562	0.47	T87/14	0.84	T87/61	1.51
T87/49-1	1.23	T83/23	0.86	T87/132	1.42	M51-3-562	0.72	T87/14	0.85	T87/61	0.86
T87/49-10	0.86	T83/23	1.63	M51-3-569	1.51	M51-3-562	1.20	T87/14	1.47	T87/61	0.96
T87/49-14	1.22	T83/23	2.11	M51-3-569	0.46	M51-3-563	1.27	T87/14	1.61	T87/61	0.79
T87/49	1.38	T83/23	1.24	M51-3-569	1.15	M51-3-563	0.94	T87/14	0.74	T87/61	1.45
T87/49	1.19	T83/23	1.69	M51-3-569	0.14	M51-3-563	0.98	T87/14	1.62	T87/61	1.32
T87/49	1.03	T83/23	1.29	M51-3-569	0.95	M51-3-563	2.29	T87/14	0.71	T87/61	0.91
T87/49	1.99	T83/23	1.34	M51-3-569	0.98	M51-3-563	1.55	T87/14	0.72	T87/61	1.40
T87/49	1.96	T83/23	1.64	M51-3-569	1.14	M51-3-563	0.86	T83/63	1.54	T87/61	1.51
T87/49	1.54	T83/23	1.77	M51-3-569	1.25	M51-3-563	1.19	T83/63	1.41	T87/61	1.45
T87/49	1.97	T83/23	1.72	M51-3-569	0.80	M51-3-563	1.02	T83/63	1.07	T87/61	1.27
T87/49	1.32	T83/23	1.52	M51-3-569	1.83	M51-3-563	0.98	T83/63	0.49	T87/61	1.05
T87/49	0.46	T83/23	1.93	M40-4-88-1	1.10	M51-3-563	0.83	T83/63	1.28	T87/61	0.76
T87/49	1.20	T83/23	1.13	M40-4-88-1	0.95	M51-3-563	0.66	T83/63	1.69	T87/61	1.28
T87/49	1.49	T83/23	1.23	M40-4-88-1	0.72	M51-3-563	1.03	T83/63	1.01	T87/61	1.47
T87/49	1.25	T83/23	1.23	M40-4-88-1	1.36	M51-3-563	1.76	T83/63	1.34		
T87/49	0.94	T83/23	1.20	M40-4-88-1	1.57	M51-3-563	0.62	T83/63	1.45		

[a]Samples measured for paired δ^{13}C-Mg/Ca analyses are listed with an additional number, matching the sample name from Table 6.

and Lea, 1996; *Bijma et al.*, 1998] The used size range for this study (250–400 μm) can explain a range in oxygen isotopes of 0.3‰ [*Kroon and Darling*, 1995]. An ontogenetic effect on the oxygen isotopes could, therefore, explain 2.2 to 3.9% of the measured 4 σ variability as measured in this study. A possible ontogenetic overprint on the seasonality reconstruction should, therefore, be kept in mind when interpreting single-specimen δ^{18}O variability.

[31] The impact of ontogenetic effects on δ^{18}O in foraminifera on paleoclimate reconstructions has been stipulated by *Spero and Lea* [1996]. These ontogenetic effects may also influence the Mg/Ca distribution in foraminifera and can be divided in two components, namely the formation of a final layer of thick calcite enveloping the whole test (GAM-calcite) at the end of the foraminifers live cycle and a decreasing trend in trace metals and stable isotopes with test size [*Nürnberg et al.*, 1996; *Bijma et al.*, 1998]. Measurements of GAM calcite in *G. sacculifer* indicate a decrease in Mg/Ca values after calcification of gametogenic calcite, in line with the decreasing trend with test size [*Bijma et al.*, 1998; *Dueñas-Bohórquez et al.*, 2009]. Observed intratest variability shows a decrease in Mg/Ca values with chamber position in the test (Figure 8). An analysis of variance (ANOVA) was conducted to assess whether this trend was significant. Results show that the mean values for the last 3 chambers are significantly different ($F = 7.028$ (20), $p < 0.05$). Furthermore, it is shown that the difference between the final chamber (F) and the F-1 and F-2 chambers is significant ($t = 4.59(26)$, $p < 0.05$), while the difference between the F-1 and F-2 chambers is not ($t = -0.647$ (16), $p > 0.05$). The significant decrease in Mg/Ca values would imply colder temperatures with increasing test size. This trend of decreasing temperatures is also seen in oxygen isotopes from symbiont bearing planktonic species *G. siphonifera* [*Bijma et al.*, 1998], suggesting that ontogenetic effects are linked to the intratest variability in Mg/Ca from *G. ruber*. The

Table 9. Calculated Correlation Coefficients (r) and Their Significance Level When Comparing Measured $\delta^{13}C$ and $\delta^{18}O$ Values of Individual Foraminifera for Each Station[a]

Sample	r	Significance
T86/11S	0.078	0.70
T87/132	−0.368	0.22
T87/114	−0.617	0.043
M40-88-1	−0.477	0.072
T87/83	−0.425	0.29
T87/61	−0.312	0.32
T87/49	−0.228	0.19
T87/30	0.240	0.43
M51-3-562	0.603	0.049
T87/14	0.018	0.97
T87/63	0.058	0.83
M51-3-563	0.470	0.24
T83/23	0.525	0.002
M51-3-569	0.312	0.38
Mediterranean	0.115	0.12

[a]Pearson's r values are calculated, since $\delta^{13}C$ and $\delta^{18}O$ distributions are not deviating from normality.

magnitude (9.8°C) of the intratest variability is, however, larger than any variation in temperature or seawater chemistry encountered during the foraminifers life cycle. The intratest variability is, therefore, probably caused by differences in Mg/Ca incorporation with each ontogenetic stage of *G. ruber*.

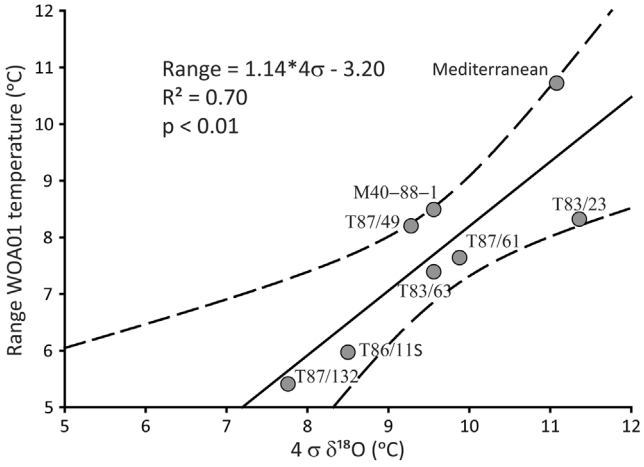

Figure 7. Four standard deviations of $\delta^{18}O$-derived temperatures versus the range (max-min) in WOA01 temperature for each sample location with 95% confidence limit of the standard deviation being less than 2°C. The Mediterranean data point is obtained by combining all measured $\delta^{18}O$ data from the Mediterranean box cores, including stations with too large confidence limits for the standard deviations, and comparing them to the combined database temperatures of those same box cores. This results in all other data plotted in Figure 7 also being included in the Mediterranean data point, potentially biasing the independency of this point. The correlation coefficient is significant at the 99% level ($p < 0.01$). The dotted lines represent the 95% confidence limits of the regression line but do not include the 95% confidence interval as calculated for each site in Table 2.

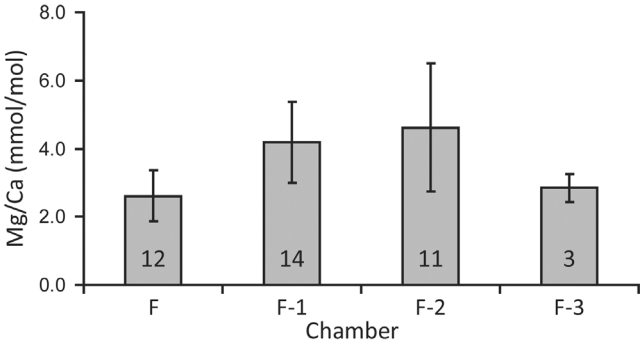

Figure 8. Mg/Ca intratest variation for site T86/11S. Chambers are numbered from the final (F) chamber downward in the spiral. The number in each column represents the amount of individual foraminifera measured for the chamber average. Error bars are based on the variability, expressed as a standard deviation, between the measurements of single chambers.

This is, however, not affecting the reconstruction of seasonality, since we picked from a size fraction which is sufficiently small (250–400 μm) to exclude any major ontogenetic effect on the average single-specimen Mg/Ca-derived temperatures.

5.2.5. Natural Variability

[32] Natural variability is here used to describe variation in $\delta^{18}O$ caused by unknown (biologically controlled) mechanisms within the calcification process, and may have an additional effect on the measured $\delta^{18}O$ variability. If natural variability is for instance 0.3‰, then every measured $\delta^{18}O$ value actually falls within a 0.3‰ range from the measured value and, therefore, introduces an additional uncertainty. Knowledge on the amplitude of natural variability within one population of foraminifera is, therefore, of vital importance for interpreting the measured standard deviations. Independent information on natural variability from the current data set cannot be obtained, since this data is generated from a series of core top samples. We therefore used the data of *Russell and Spero* [2000] instead. They measured single-specimen $\delta^{18}O$ on *G. ruber* tests from a series of sediment traps in the eastern equatorial Pacific and assume that natural variability is primarily species specific. This is realistic since natural variability is probably largely biologically controlled. The standard deviation over a 1.5–3 day period in the Pacific sediment trap is 0.87°C (based on $\delta^{18}O$) and could potentially explain 25–45% of the measured standard deviations in our samples.

[33] Natural variability in Mg/Ca could have similar effects as it does for $\delta^{18}O$, and therefore may have an important impact on the measured Mg/Ca variability. To make an assessment on the natural variability within a population of *G. ruber* we used the Mg/Ca measurements of a plankton pump data set from *Sadekov et al.* [2008]. This data set has a standard deviation of 1.9°C. Hence, natural variability could potentially explain 52% (T87/49) and 63% (T86/11S) of the measured standard deviation, again assuming that the values for natural variability are species specific.

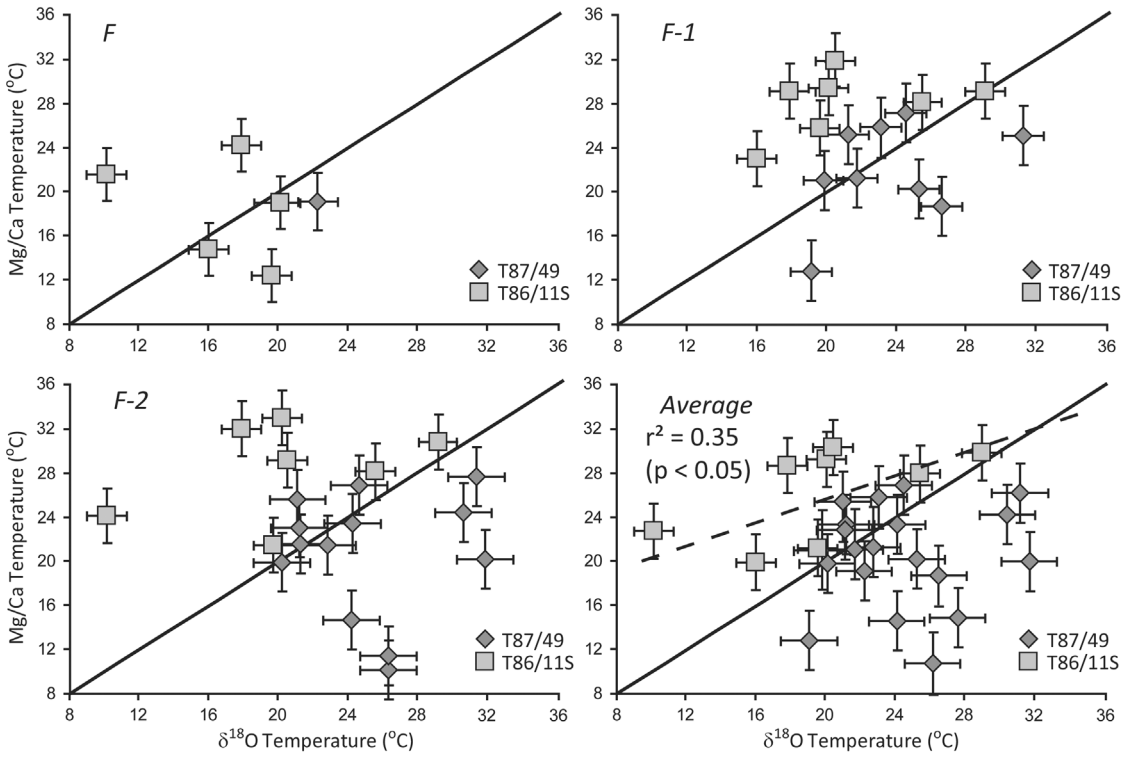

Figure 9. The δ^{18}O- versus Mg/Ca-derived temperatures for sites T87/49 and T86/11S. Error bars include temperature uncertainties caused by salinity, carbonate ion concentrations, and natural variability. Final chamber (F), second last chamber (F-1), and third last chamber (F-2) Mg/Ca-derived temperatures are based on one chamber of a single foraminifer only. Mg/Ca-derived temperatures for the average are based on measurements on multiple chambers of a single foraminifer. The dashed line in the average plot represents the regression line for the T86/11S samples. The correlation coefficient is significant at the 95% level ($p < 0.05$).

5.3. The δ^{18}O- and Mg/Ca-Derived Temperature Comparison

[34] Despite uncertainties, single-specimen δ^{18}O and Mg/Ca variability can be used for reconstructing sea surface temperature seasonality, as indicated by the good correlation between measured variability and WOA01 temperature data. The fact that our data are derived from the same individual foraminiferal test also allows calculating the linear correlation coefficient between δ^{18}O- and Mg/Ca-derived temperatures. Theoretically, if both proxies would record temperature of the ambient water perfectly, the relation should be close to 1. No clear linear correlation is, however, observed when comparing δ^{18}O- and Mg/Ca-derived temperatures of core T86/11S and T87/49, implying an offset in one or both of the temperature proxies (Figure 9). One of the causes of this offset could be the position of T86/11S at the boundary of two major water masses in the North Atlantic, causing an error in the used $\delta^{18}O_w$ for calculating the oxygen isotope–derived temperatures (Figure 1). Values for T86/11S, however, appear to show a slight significant positive trend (dashed line in Figure 9).

[35] Reconstructed δ^{18}O-derived temperatures for site T87/49 did, however, record annual conditions as well as the seasonal temperature contrast (Figures 5 and 7). The question of what is causing this apparent offset between individual δ^{18}O- and Mg/Ca-derived temperatures, therefore, still remains. Here, we propose two possible causes. First, the Mg/Ca measurements are derived from laser ablation ICP-MS analyses on foraminiferal chambers and therefore represent point measurements. While the δ^{18}O composition of the foraminiferal shell is measured by dissolving the entire shell and represents an integrated values for the whole foraminifer. A direct comparison between these values could thus introduce an offset and/or variability between both temperature proxies. Second, single-specimen δ^{18}O and Mg/Ca variability is influenced by other parameters than temperature alone, as we already argued. Two of the discussed parameters, salinity and $[CO_3^{2-}]$, cause a systematic offset. These offsets are, however, not the same for δ^{18}O and Mg/Ca. As already shown, an 0.1 increase in salinity will cause an uncertainty of 0.12 and 0.28°C in δ^{18}O- and Mg/Ca-derived temperatures, respectively, causing a slight offset between both temperatures. An increase of 10 μmol/kg in $[CO_3^{2-}]$ will cause a 0.09°C increase and a 0.27°C decrease in δ^{18}O- and Mg/Ca-derived temperatures, respectively, causing a 0.36°C per 10 μmol/kg change. The mechanism behind natural variability remains unknown, causing the offset produced by natural variability to be unpredictable. In a worst case

scenario natural variability could cause an offset of 2.8°C (0.87°C for δ^{18}O and 1.9°C for Mg/Ca). All these factors combined could explain the large offset seen in Figure 9.

6. Conclusions

[36] The results show that averaged δ^{18}O-derived temperatures measured on single-specimen *G. ruber* test correspond to average annual temperatures, with the perquisite there is no seasonal bias at the sample location. Measured intertest variations in both δ^{18}O and Mg/Ca of single-specimen *G. ruber* tests largely concur with observed annual temperature variability (seasonality) if enough specimens are measured (i.e., confidence limits of the standard deviations <2°C). This suggests that both proxies of single-specimen *G. ruber* tests independently record seasonality. But it remains largely unclear why the two temperature proxies from the same individual specimen differ. A possible explanation could be that seasonal changes in salinity, carbonate ion concentration and especially natural variability are causing a major part of the measured offset. Accurate reconstruction of seasonality, therefore, hinges on our ability to quantify these effects in the past. The biological mechanisms behind natural variability are still unknown and could be related to changes in the foraminifer's microenvironment. An assessment of these mechanisms is, therefore, of vital importance for reconstructing natural variability and, therefore, an accurate reconstruction of seasonality.

[37] **Acknowledgments.** We would like to thank Simon Troelstra, Lia Auliaherliaty, and Karl Emeis for providing samples. We appreciate the assistance of Paul Mason and Gijs Nobbe with laser ablation analyses. Hans de Moel is thanked for his help with the statistical data treatment. Further, we want to thank Martin Ziegler and three anonymous reviewers for providing constructive comments on the manuscript and an earlier draft. This research is funded by the Utrecht University, the Vrije Universiteit Amsterdam, and the Darwin Centre for Geobiology projects "Assessing the seasonality evolution in the Mediterranean Sea: calibration of carbonate-based proxies and application in selected time slices" and "Biological validation of proxies for temperature, salinity, oxygenation and pCO_2 based on experimental evidence using benthic foraminiferal cultures."

References

Anand, P., and H. Elderfield (2005), Variability of Mg/Ca and Sr/Ca between and within the planktonic foraminifers *Globigerina bulloides* and *Globorotalia truncatulinoides*, *Geochem. Geophys. Geosyst.*, *6*, Q11D15, doi:10.1029/2004GC000811.

Anand, P., H. Elderfield, and M. H. Conte (2003), Calibration of Mg/Ca thermometry in planktonic foraminifera from a sediment trap time series, *Paleoceanography*, *18*(2), 1050, doi:10.1029/2002PA000846.

Bárcena, M. A., J. A. Flores, F. J. Sierro, M. Pérez-Folgado, J. Fabres, A. Calafat, and M. Canals (2004), Planktonic response to main oceanographic changes in the Alboran Sea (western Mediterranean) as documented in sediment traps and surface sediments, *Mar. Micropaleontol.*, *53*, 423–445, doi:10.1016/j.marmicro.2004.09.009.

Barker, S., M. Greaves, and H. Elderfield (2003), A study of cleaning procedures used for foraminiferal Mg/Ca paleothermometry, *Geochem. Geophys. Geosyst.*, *4*(9), 8407, doi:10.1029/2003GC000559.

Bemis, B. E., H. J. Spero, J. Bijma, and D. W. Lea (1998), Reevaluation of the oxygen isotopic composition of planktonic foraminifera: Experimental results and revised paleotemperature equations, *Paleoceanography*, *13*, 150–160, doi:10.1029/98PA00070.

Bijma, J., C. Hemleben, B. T. Huber, H. Erlenkeuser, and D. Kroon (1998), Experimental determination of ontogenetic stable isotope variability in two morphotypes of *Globigerinella siphonifera* (d'Orbigny), *Mar. Micropaleontol.*, *35*, 141–160, doi:10.1016/S0377-8398(98)00017-6.

Billups, K., and H. Spero (1996), Reconstructing the stable isotope geochemistry and paleotemperatures of equatorial Atlantic during the last 150,000 years: Results from individual foraminifera, *Paleoceanography*, *11*, 217–238, doi:10.1029/95PA03773.

Bluman, A. G. (2004), *Elementary Statistics: A Step by Step Approach*, 810 pp., McGraw-Hill, New York.

Conkright, M. E., R. A. Locarnini, H. E. Garcia, T. D. O'Brien, T. P. Boyer, C. Stephens, and J. I. Antonov (2002), World Ocean Atlas 2001: Objective analyses, data statistics, and figures, CD-ROM documentation, *Internal Rep. 17*, Natl. Oceanogr. Data Cent., Silver Spring, Md.

Dekens, P. S., D. W. Lea, D. K. Pak, and H. J. Spero (2002), Core top calibration of Mg/Ca in tropical foraminifera: Refining paleotemperature estimation, *Geochem. Geophys. Geosyst.*, *3*(4), 1022, doi:10.1029/2001GC000200.

deMenocal, P., J. Ortiz, T. Guilderson, and M. Sarnthein (2000), Coherent high- and low-latitude climate variability during the Holocene warm period, *Science*, *288*, 2198–2202, doi:10.1126/science.288.5474.2198.

Denton, G. H., R. B. Alley, G. C. Comer, and W. S. Broecker (2005), The role of seasonality in abrupt climate change, *Quat. Sci. Rev.*, *24*, 1159–1182, doi:10.1016/j.quascirev.2004.12.002.

De Rijk, S., S. R. Troelstra, and E. J. Rohling (1999), Benthic foraminiferal distribution in the Mediterranean Sea, *J. Foraminiferal Res.*, *29*, 93–103.

Dueñas-Bohórquez, A., E. S. da Rocha, A. Kuroyanagi, J. Bijma, and G.-J. Reichart (2009), Effect of salinity and seawater calcite saturation state on Mg and Sr incorporation in cultured planktonic foraminifera, *Mar. Micropaleontol.*, *73*(3–4), 178–189, doi:10.1016/j.marmicro.2009.09.002.

Elderfield, H., and G. Ganssen (2000), Past temperature and δ^{18}O of surface waters inferred from foraminiferal Mg/Ca ratios, *Nature*, *405*, 442–445, doi:10.1038/35013033.

Epstein, S., R. Buchsbaum, H. Lowenstam, and H. C. Urey (1951), Carbonate-water isotopic temperature scale, *Geol. Soc. Am. Bull.*, *62*, 417–426, doi:10.1130/0016-7606(1951)62[417:CITS]2.0.CO;2.

Ganssen, G. M., and D. Kroon (2000), The isotopic signature of planktonic foraminifera from NE Atlantic surface sediments: Implications for the reconstructions of past oceanic conditions, *J. Geol. Soc.*, *157*, 693–699, doi:10.1144/jgs.157.3.693.

Ganssen, G. M., G. J. A. Brummer, S. J. A. Jung, D. Kroon, and F. J. C. Peeters (2005), The oxygen isotope composition in planktic foraminifera shells as recorder of maximum seasonal SST variation, *Geophys. Res. Abstr.*, *7*, 01775.

Goyet, C., R. J. Healy, and J. Ryan (2000), Global distribution of total inorganic carbon and total alkalinity below the deepest winter mixed layer depths, *Rep. ORNL/CDIAC-127*, Carbon Dioxide Inf. Anal. Cent., Oak Ridge Natl. Lab., Oak Ridge, Tenn.

Hathorne, E. C., R. H. James, and R. S. Lampitt (2009), Environmental versus biomineralization controls on the intratest variation in the trace element composition of the planktonic foraminifera *G. inflata* and *G. scitula*, *Paleoceanography*, *24*, PA4204, doi:10.1029/2009PA001742.

Hemleben, C. (2002), Short cruise report, R.V. *Meteor*, cruise M51-3, 14 Nov.–10 Dec. 2001, Inst. of Oceanogr., Univ. of Hamburg, Hamburg, Germany. (Available at http://www.ifm.zmaw.de/fileadmin/files/leitstelle/meteor/M51/M51-3-scr.pdf)

Hemleben, C., M. Spindler, and O. R. Anderson (1989), *Modern Planktonic Foraminifera*, 363 pp., Springer, New York.

Hopkins, T. S. (1991), The GIN sea—A synthesis of its physical oceanography and literature review 1972–1985, *Earth Sci. Rev.*, *30*, 175–318, doi:10.1016/0012-8252(91)90001-V.

Hübscher, C. (2002), Short cruise report, R.V. *Meteor*, cruise M52-2, 4–25 Feb. 2002, Inst. of Oceanogr., Univ. of Hamburg, Hamburg, Germany. (Available at http://www.ifm.zmaw.de/fileadmin/files/leitstelle/meteor/M52/M52-2-SCR.pdf)

Hurrell, J. W. (1995), Decadal trends in the North Atlantic Oscillation: Regional temperatures and precipitation, *Science*, *269*, 676–679, doi:10.1126/science.269.5224.676.

Hut, G. (1987), Consultants' Group Meeting on Stable Isotope Reference Samples for Geochemical and Hydrological Investigations, report to the Director General, 42 pp., Int. At. Energy Agency, Vienna.

Kisakürek, B., A. Eisenhauer, F. Böhm, D. Garbe-Schönberg, and J. Erez (2008), Controls on shell Mg/Ca and Sr/Ca in cultured planktonic foraminiferan, *Globigerinoides ruber* (white), *Earth Planet. Sci. Lett.*, *273*, 260–269, doi:10.1016/j.epsl.2008.06.026.

Koutavas, A., P. B. deMenocal, G. C. Olive, and J. Lynch-Stieglitz (2006), Mid-Holocene El Niño–Southern Oscillation (ENSO) attenuation revealed by individual foraminifera in eastern tropical Pacific sediments, *Geology*, *34*, 993–996, doi:10.1130/G22810A.1.

Kroon, D., and K. Darling (1995), Size and upwelling control of stable isotope composition of *Neogloboquadrina dutertrei* (d'Orbigny), *Globigerinoides ruber* (d'Orbigny) and *Globigerina bulloides* d'Orbigny: Examples from the Panama Basin and Arabian Sea, *J. Foraminiferal Res.*, *25*, 39–52, doi:10.2113/gsjfr.25.1.39.

Lea, D. W., T. A. Mashiotta, and H. J. Spero (1999), Controls on magnesium and strontium uptake in planktonic foraminifera determined by live culturing, *Geochim. Cosmochim. Acta*, *63*, 2369–2379, doi:10.1016/S0016-7037(99)00197-0.

Lewis, E., and D. Wallace (1998), Program developed for CO_2 system calculations, *Rep. ORNL/CDIAC-105*, Carbon Dioxide Inf. Anal. Cent., Oak Ridge Natl. Lab, Oak Ridge, Tenn.

Millot, C. (1987), Circulation in the western Mediterranean, *Oceanol. Acta*, *10*, 143–149.

Nürnberg, D., J. Bijma, and C. Hemleben (1996), Assessing the reliability of magnesium in foraminferal calcite as a proxy for water mass temperatures, *Geochim. Cosmochim. Acta*, *60*, 803–814, doi:10.1016/0016-7037(95)00446-7.

O'Neil, J. R., R. N. Clayton, and T. K. Mayeda (1969), Oxygen isotope fractionation in divalent metal carbonates, *J. Chem. Phys.*, *51*, 5547–5558, doi:10.1063/1.1671982.

Ottens, J. J. (1991), Planktonic foraminifera as North Atlantic water mass indicators, *Oceanol. Acta*, *14*(2), 123–140.

Ovchinnikov, I. M. (1966), Circulation in the surface and intermediate layers of the Mediterranean, *Oceanology*, Engl. Transl., *6*, 48–59.

Pierre, C. (1999), The oxygen and carbon isotope distribution in the Mediterranean water masses, *Mar. Geol.*, *153*, 41–45, doi:10.1016/S0025-3227(98)00090-5.

Pujol, C., and C. Vergnaud-Grazzini (1995), Distribution patterns of live planktic foraminifers as related to regional hydrography and productive systems of the Mediterranean Sea, *Mar. Micropaleontol.*, *25*, 187–217, doi:10.1016/0377-8398(95)00002-I.

Reichart, G.-J., F. Jorissen, P. Anschutz, and P. R. D. Mason (2003), Single foraminiferal test chemistry records the marine environment, *Geology*, *31*, 355–358, doi:10.1130/0091-7613(2003)031<0355:SFTCRT>2.0.CO;2.

Rohling, E. J. (1999), Environmental control on Mediterranean salinity and $\delta^{18}O$, *Paleoceanography*, *14*, 706–715, doi:10.1029/1999PA900042.

Rohling, E. J., and G. R. Bigg (1998), Paleosalinity and $\delta^{18}O$: A critical assessment, *J. Geophys. Res.*, *103*, 1307–1318, doi:10.1029/97JC01047.

Rossignol-Strick, M. (1985), Mediterranean Quaternary sapropels, an immediate response of the African monsoon to variation of insolation, *Palaeogeogr. Palaeoclimatol. Palaeoecol.*, *49*, 237–263, doi:10.1016/0031-0182(85)90056-2.

Rupke, N. A., D. J. Stanley, and R. Stuckenrath (1974), Late Quaternary rates of abyssal mud deposition in the western Mediterranean Sea, *Mar. Geol.*, *17*, M9–M16, doi:10.1016/0025-3227(74)90039-5.

Russell, A. D., and H. J. Spero (2000), Field examination of the oceanic carbonate ion effect on stable isotopes in planktonic foraminifera, *Paleoceanography*, *15*, 43–52, doi:10.1029/1998PA000312.

Russell, A. D., B. Hönisch, H. J. Spero, and D. W. Lea (2004), Effects of seawater carbonate ion concentration and temperature on shell U, Mg, and Sr in cultured planktonic foraminifera, *Geochim. Cosmochim. Acta*, *68*, 4347–4361, doi:10.1016/j.gca.2004.03.013.

Rutten, A., G. J. de Lange, P. Ziveri, J. Thomson, P. J. M. van Santvoort, S. Colley, and C. Corselli (2000), Recent terrestrial and carbonate fluxes in the pelagic eastern Mediterranean; a comparison between sediment trap and surface sediment, *Palaeogeogr. Palaeoclimatol. Palaeoecol.*, *158*, 197–213, doi:10.1016/S0031-0182(00)00050-X.

Sadekov, A., S. Eggins, P. De Deckker, and D. Kroon (2008), Uncertainties in seawater thermometry deriving from intratest and intertest Mg/Ca variability in *Globigerinoides ruber*, *Paleoceanography*, *23*, PA1215, doi:10.1029/2007PA001452.

Schiebel, R., and C. Hemleben (2005), Modern planktic foraminifera, *Palaeontol. Z.*, *79*, 135–148.

Schilman, B., M. Bar-Matthews, A. Almogi-Labin, and B. Luz (2001), Global climate instability reflected by eastern Mediterranean marine records during the late Holocene, *Palaeogeogr. Palaeoclimatol. Palaeoecol.*, *176*, 157–176, doi:10.1016/S0031-0182(01)00336-4.

Schmidt, G. A., G. R. Bigg, and E. J. Rohling (1999), Global Seawater Oxygen-18 Database, http://data.giss.nasa.gov/o18data/, Goddard Inst. for Space Stud., NASA, New York.

Shackleton, N. J. (1974), Attainment of isotopic equilibrium between ocean water and benthonic foraminifera genus *Uvigerina*: Isotopic changes in the oceans during the last glacial, *Colloq. Int. C.N.R.S.*, *219*, 203–209.

Spero, H. J. (1992), Do planktic foraminifera accurately record shifts in the carbon isotopic composition of seawater ΣCO_2, *Mar. Micropaleontol.*, *19*, 275–285, doi:10.1016/0377-8398(92)90033-G.

Spero, H. J., and D. W. Lea (1993), Intraspecific stable isotope variability in the planktic foraminifera *Globigerinoides sacculifer*: Results from laboratory experiments, *Mar. Micropaleontol.*, *22*, 221–234, doi:10.1016/0377-8398(93)90045-Y.

Spero, H. J., and D. W. Lea (1996), Experimental determination of stable isotope variability in *Globigerina bulloides*: Implications for paleoceanographic reconstructions, *Mar. Micropaleontol.*, *28*, 231–246, doi:10.1016/0377-8398(96)00003-5.

Spero, H. J., and D. F. Williams (1988), Extracting environmental information from planktonic foraminiferal $\delta^{13}C$ data, *Nature*, *335*, 717–719, doi:10.1038/335717a0.

Spero, H. J., and D. F. Williams (1989), Opening the carbon isotope "vital effect" black box: 1. Seasonal temperatures in the euphotic zone, *Paleoceanography*, *4*, 593–601, doi:10.1029/PA004i006p00593.

Spero, H. J., J. Bijma, D. W. Lea, and B. E. Bemis (1997), Effect of seawater carbonate concentration on foraminiferal carbon and oxygen isotopes, *Nature*, *390*, 497–500, doi:10.1038/37333.

Tadjiki, S., and H. N. Erten (1994), Radiochronology of sediments from the Mediterranean Sea using natural ^{210}Pb and fallout ^{137}Cs, *J. Radioanal. Nucl. Chem.*, *181*, 447–459, doi:10.1007/BF02037651.

Ziegler, M., D. Nürnberg, C. Karas, R. Tiedemann, and L. J. Lourens (2008), Persistent summer expansion of the Atlantic Warm Pool during glacial abrupt cold events, *Nat. Geosci.*, *1*, 601–605, doi:10.1038/ngeo277.

S. J. A Jung and D. Kroon, School of GeoSciences, Grant Institute, University of Edinburgh, West Mains Road, Edinburgh EH9 3JW, UK.

G.-J. Reichart and J. C. Wit, Department of Geochemistry, Faculty of Geosciences, Utrecht University, Budapestlaan 4, NL-3584 CD Utrecht, Netherlands. (j.wit@geo.uu.nl)